

Status and latest results from the NA62 Experiment at CERN

Patrizia Cenci^a

^aINFN Perugia, Via A. Pascoli, 06123 Perugia, Italy

Abstract

The ultra-rare decays $K \rightarrow \pi \nu \bar{\nu}$ are excellent processes to make tests of new physics at the highest energy scale complementary to LHC, thanks to their theoretically clean predictions. The NA62 experiment at the CERN SPS aims to collect about 100 $K^+ \rightarrow \pi^+ \nu \bar{\nu}$ events in two years of data taking, keeping the background at 10% level. A rich physics program is accessible to NA62, in addition to the main goal. A precise measurement of the helicity-suppressed ratio R_K of the $K^\pm \rightarrow e \nu_e$ and $K^\pm \rightarrow \mu \nu_\mu$ decay rates has already been performed, using data collected at an early stage of the experiment. The result agrees with the Standard Model expectations. A description of the R_K measurement, the physics prospects and the status of the NA62 experiment will be presented in this paper.

Keywords: Decays of K mesons, Electroweak Interactions, Standard Model, Cabibbo-Kobayashi & Maskawa (CKM) matrix, Supersymmetric models

1. Introduction

Quests for ultra-rare or forbidden processes as well as precision measurements of electroweak parameters, performed to reveal deviations from very accurate Standard Model (SM) predictions, are powerful tools in seeking new physics (NP) beyond the SM. Independent techniques are exploited to address frontier research in particle physics. The precise measurements of rare processes attained with intense beams are an excellent indirect mode of looking into particle physics at the highest energy scales in a coordinated and complementary way with respect to the direct investigation of large mass scales achieved at the LHC. Both those methods are essential to accomplish a deep investigation of fundamental interactions. Kaon physics is a suitable example of the former approach.

NA62 [1][2] is the last generation experiment with kaons at CERN. Its main goal is to collect about 100 ultra-rare $K^+ \rightarrow \pi^+ \nu \bar{\nu}$ events with 10% of background in two years of data taking, foreseen in 2014–15.

At present, the construction of the experimental apparatus is almost completed. A commissioning run

© CERN for the benefit of the NA62 Collaboration.

is taking place in 2012, with a subset of the detector and of the data acquisition and read-out systems. At an early stage of the NA62 project, in 2007–08, physics data have been collected using an optimized kaon beam line and the former NA48/2 detector [3] to measure the ratio $R_K = \Gamma(K^\pm \rightarrow e \nu_e) / \Gamma(K^\pm \rightarrow \mu \nu_\mu) = \Gamma(K_{e2}) / \Gamma(K_{\mu 2})$ of the K_{e2} and $K_{\mu 2}$ decay rates [4][5]. The result is the most precise R_K measurement to date and agrees with the SM predictions.

The role of the golden $K \rightarrow \pi \nu \bar{\nu}$ decays in seeking NP beyond the SM is summarized in Section 2; the NA62 experimental technique and the detector are discussed in Section 3 and the R_K measurement is described in Section 4.

2. The rare decays $K \rightarrow \pi \nu \bar{\nu}$

The present collider searches at high transverse momenta exclude wide regions of the parameter space for NP thus increasing the importance of the study of rare processes sensitive to very high energy.

This is true, in particular, for the $K \rightarrow \pi \nu \bar{\nu}$ decays, whose SM predictions are known with very high

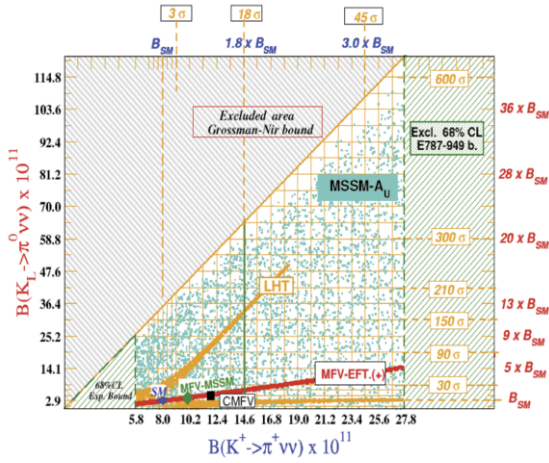


Fig. 1. Correlation between the branching ratios of the pair of decays $K \rightarrow \pi \nu \bar{\nu}$ showing the predictions of SM and of some NP models [8].

precision [6]. The branching ratio (BR) expectation of the CP-violating $K^0 \rightarrow \pi^0 \nu \bar{\nu}$ channel is:

$$\text{BR}(K^0 \rightarrow \pi^0 \nu \bar{\nu}) = (0.243 \pm 0.039 \pm 0.006) \times 10^{-10}.$$

The BR prediction of the charged mode is:

$$\text{BR}(K^+ \rightarrow \pi^+ \nu \bar{\nu}) = (0.781 \pm 0.075 \pm 0.029) \times 10^{-10}.$$

In both cases, the first error summarises the parametric uncertainty, the second one the remaining theoretical error. The extremely high precision of these expected BR values is due to many reasons: the processes are well described in terms of short distance dynamics and only arise at loop level, with top-quark loops dominating the matrix elements; the electroweak amplitudes are predicted at a high degree of accuracy; the hadronic matrix elements are easily obtained from the well-known BR of the semi-leptonic K_{e3} decays, via isospin symmetry. The main uncertainties are due to the knowledge of the CKM matrix elements. The irreducible theoretical error for the BR of the charged mode is less than 2%.

Processes mediated by flavour-changing neutral currents (FCNC) are suppressed in the SM by the GIM mechanisms [7]. Further suppression can originate from hierarchies in CKM matrix or helicity. In some models of NP these suppression mechanisms are lifted, leading to a potentially large enhancement of the SM rates. However, even small deviations from the SM can reveal the presence of NP.

Among several FCNC decays of K and B mesons, the $K \rightarrow \pi \nu \bar{\nu}$ modes play a key role in seeking NP beyond the SM. This is clear from Figure 1, which reproduces the BR values predicted by the SM and by some models of NP [8]. Apart from establishing a direct signal of NP, the correlation of the BR of the two modes can be effectively utilized to probe the

flavour structure of NP theories and, therefore, to distinguish among different classes of NP scenarios. The exclusion regions given by the Grossman-Nir consistency conditions [9], limiting the BR ratio of the two decay modes, and by the only measurement of the charged mode [10] are reproduced in Figure 1. The grid in the allowed region is a function of the theoretical errors on the SM prediction.

The CP-violating neutral $K^0 \rightarrow \pi^0 \nu \bar{\nu}$ decay has not been revealed yet. An upper limit to the BR [11] was posed by the E391a collaboration at KEK (Japan):

$$\text{BR}(K^0 \rightarrow \pi^0 \nu \bar{\nu}) < 260 \times 10^{-10} \quad (90\% \text{ C.L.}).$$

The next generation KOTO project [12] at J-PARC (Japan) aims at observing the process for the first time, achieving the SM sensitivity. The first physics run of this experiment is foreseen in 2013.

The only $\text{BR}(K^+ \rightarrow \pi^+ \nu \bar{\nu})$ measurement is based on 7 events observed by the stopping-kaon E959 and E787 experiments at BNL (US) [10]. The result is compatible with the SM prediction within the errors:

$$\text{BR}(K^+ \rightarrow \pi^+ \nu \bar{\nu}) = (1.73^{+1.15}_{-1.05}) \times 10^{-10}.$$

An accuracy of about 10% should be achieved to make the BR measurement of the charged mode an effective test of new physics. This is, indeed, the main purpose of the NA62 experiment at the CERN SPS, which aims to collect about 100 charged decays in two years of physics data taking, keeping the background contamination at the 10% level.

The new ORKA experiment at FNAL (US) aims at detecting about 1000 $K^+ \rightarrow \pi^+ \nu \bar{\nu}$ decays [13]. The proposal has been submitted in 2011 and received the Stage 1 approval from the FNAL directorate.

3. The NA62 Experiment

The NA62 goal of detecting about 100 $K^+ \rightarrow \pi^+ \nu \bar{\nu}$ events with 10% background implies to collect more than 10^{13} K decays with a background rejection factor of at least 10^{12} , assuming a signal acceptance of 10%, which is well within the reach of the experiment.

The experimental method relies on exploiting a decay-in-flight technique with an intense charged kaon beam at high energy. This requires a beam of un-separated charged hadrons (with 6% K^+), a long decay region with an extended detector and the event-by-event measurement of kaon momenta. Positive charged kaons will be used in order to get, at the same proton energy and flux, higher kaon fluxes and lower pion background.

The NA62 analysis strategy is based on the accurate kinematic reconstruction of all the particles

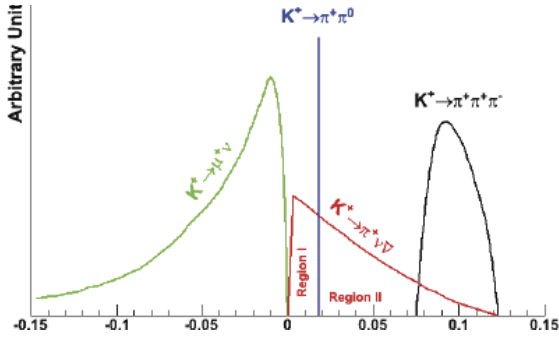


Fig. 2. Squared missing mass of the signal and the main K^+ decays.

detected in the event to disentangle the signal from the huge amount of background processes, a precise timing to associate correctly the π^+ with the parent K^+ , a system of efficient vetoes to reject events with γ and μ in the final state, effective particle identification systems to identify K^+ among other particles of the intense hadron beam and to distinguish π^+ from μ^+ and e^+ in the final states.

3.1. The Experimental Technique

The $K^+ \rightarrow \pi^+ \nu \bar{\nu}$ signal definition relies on the reconstruction of the event kinematics and is based on the squared missing mass variable, m_{miss}^2 , defined as the square of the difference of the 4-momenta of the K^+ and of the downstream track, in the π^+ hypothesis: $m_{miss}^2 = (P_K - P_{\pi})^2$.

Figure 2 shows the m_{miss}^2 distribution for the signal and the main K^+ decays, accounting for more than 90% of the total background. The $K^+ \rightarrow \pi^+ \pi^0$ peak clearly identifies two different m_{miss}^2 regions, Region I and II, with minimal background contamination. The residual background in those regions is due to kinematics resolution effects.

High-resolution tracking devices are needed to keep the m_{miss}^2 resolution tails as small as possible. This requires low mass and high precision detectors, installed in vacuum, in order to keep multiple scattering as low as possible. A Geant4 [14] Monte Carlo simulation of the beam tracker and the downstream spectrometer predicts kinematic rejection powers of about 10^4 and 10^5 against the $K^+ \rightarrow \pi^+ \pi^0$ (BR $\sim 21\%$) and $K^+ \rightarrow \mu^+ \nu$ (BR $\sim 64\%$) decay modes, respectively.

The K^+ decays which cannot be separated from the signal with a kinematic selection based on a m_{miss}^2 threshold, as the radiative or the semileptonic ones, account for less than 10% of the total background. An additional background rejection factor, mostly

independent from kinematics, is based on the detection of γ and μ in the final state and requires efficient veto and particle identification devices. An inefficiency of about 10^{-8} on the π^0 detection is needed for the photon veto system, driven by the $K^+ \rightarrow \pi^+ \pi^0$ background suppression. The use of a kinematic threshold does not provide a sufficient reduction of the $K^+ \rightarrow \mu^+ \nu(\gamma)$ background events. A suitable μ rejection factor is accomplished by exploiting a muon veto detector with inefficiency at the 10^{-5} level and a RICH detector distinguishing π from μ among the K^+ decay products with a μ reduction better than 10^{-2} .

A total signal acceptance of about 14.4%, summed over the two m_{miss}^2 regions, have been obtained with preliminary Monte Carlo simulations based on Geant4 [14], Geant3 [15] and Fluka [16]. This shows that the expected 10% signal acceptance is within the experiment reach, even taking into account additional losses occurring in the real data taking. The momenta of the accepted pion tracks are constrained between 15 and 35 GeV/c by the use of the RICH. While causing an important loss of the signal acceptance, the above upper momentum threshold ensures electromagnetic energy depositions of at least 40 GeV for $K^+ \rightarrow \pi^+ \pi^0$ events, thus making their rejection easier with the photon veto system. A simple counting of signal events and of many sources of background processes in the signal regions showed that the 10% background limit is achievable.

3.2. The NA62 Detector

The NA62 experiment will be housed in the CERN North Area where the previous NA48 detector [3] was installed and will exploit the same SPS extraction line and target. A new high acceptance beam line will deliver a 50 times more intense secondary beam made of positive charged hadrons, positron free, composed by 6% of K^+ . The beam particle momentum will be 75 GeV/c, with a $\pm 1\%$ spread. The expected average beam rate is about 800 MHz, integrated over an area of 14 cm².

Figure 3 shows the layout of the NA62 detector [17]. A system of sub-detectors, installed at about 170 m downstream of the target, will detect the K^+ decay products. The average integrated rate on these detectors will be about 10 MHz, mainly due to kaon decays and accidental muons. Assuming 100 days of run at 60% efficiency and 60 m decay region, the beam line will provide 5×10^{12} K^+ decays per year.

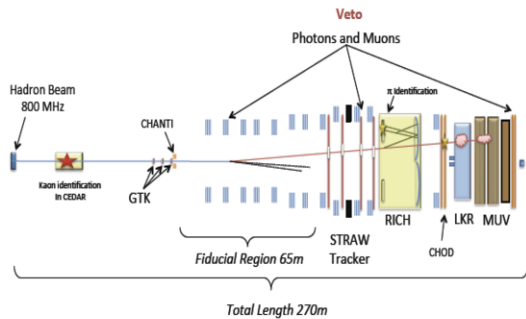


Fig. 3. Layout of the NA62 detector.

The detector and beam line installation are in progress; a commissioning run with beams will take place in fall 2012 to test the sub-detectors, the read-out and the trigger and data acquisition systems available so far, assembled together for the first time. The physics data taking is expected in 2014 and 2015, after the CERN accelerator shutdown.

Low mass and high precision tracking devices will detect the K^+ beam and the charged decay products. A beam tracker and a spectrometer downstream of the decay region will accomplish these tasks. The high beam rate requires the association of the parent K^+ with the π^+ by tight spatial and time coincidences: the beam tracker itself, together with the downstream RICH, will provide the timing of the experiment.

A beam spectrometer will measure time, direction and momentum of all the beam particle tracks at an average rate of about 800 MHz (Giga-tracker, GTK). It will stand extremely high radiation levels, comparable to those suffered by the inner layers of the LHC trackers in 10 years. The expected time resolution should be better than 200 ps. The GTK consists of 3 hybrid Si-pixel stations with dimensions matching the beam size. A Si sensor, 200 μm thick, and a read-out chip, 100 μm thick, bump bonded on the sensor, form one pixel. The time resolution measured on prototype beam tests at CERN in 2010, as well as the direction and momentum resolutions, agree with expectations.

A downstream spectrometer based on straw tubes will reconstruct coordinates and momenta of the charged particles in the decay region. The straw tubes are made of 36 μm Cu/Au-plated mylar foils, 2.1 m long, with 9.6 mm diameter. Four chambers will be placed in the same vacuum of the decay region. Each chamber is made by four planes of tubes, oriented along the x, y and ± 45 degrees directions. The old

NA48 dipole magnet, placed after the second chamber, will be used for momentum analysis. Full-length plane prototypes operating in vacuum have been tested with hadron beams at CERN. A resolution lower than 100 μm for each coordinate has been measured together with suitable efficiency, momentum and angular resolutions. Half a chamber will be tested in 2012.

Particle identification relies on two Cherenkov detectors to identify the K^+ beam particles and to distinguish μ from π among the decay products.

A CEDAR (ChErenkov Differential Counter with Achromatic Ring focus) [18], used at CERN for particle identification in the SPS secondary hadron beams, has been adapted to the NA62 needs in order to identify and tag K^+ within the 800 MHz hadron beam (KTAG). Filled with H_2 gas at a 3.85 bar nominal pressure, the KTAG will stand a K^+ rate of about 50 MHz rate (6% of the total), being insensitive to π and p. A prototype with different options of front-end and read-out electronics was tested at CERN in 2011, showing adequate efficiency and timing performance. Half of the detector will be equipped for testing in the 2012 commissioning run.

A long-focus RICH (Ring Imaging Cherenkov) detector will identify and reduce μ contaminating the π sample with inefficiency below 1% in a momentum range between 15 and 35 GeV/c. This device will measure the arrival time of charged tracks with a resolution better than 100 ps and provide trigger signals for 1-track events. A vacuum-proof vessel with cylindrical shape, diameter of about 4 m and length of about 17.5 m, will work with Neon gas at atmospheric pressure and room temperature. The Cherenkov light will be reflected by a mosaic of 20 mirrors with 17 m focal length and collected by about 2000 Hamamatsu photomultipliers (PM) with quantum efficiency and timing performances fitting the detector requirements. The PM will be housed on two disks, placed on both the sides of the vessel, at the entrance window. The results of the tests of a full-length prototype, done with hadron beams at CERN in 2007 and 2009 [19][20], showed an average μ misidentification probability better than 1% in the 15–35 GeV/c momentum range and a time resolution around 70 ps, in agreement with the expectations. The installation of the detector will start in 2013.

The detection of γ and μ among the K^+ decay products will provide additional background rejection factors, largely independent from kinematics. The photon veto system will achieve suitable suppression factors of $K^+ \rightarrow \pi^+ \pi^0$ events already at the online level, to reduce data acquisition rates. It will consist of

several devices: a system of calorimeters covering the angular region between 8.5 and 50 mrad, the Large Angle Veto (LAV); the former NA48 Liquid Krypton electromagnetic calorimeter (LKr), between 1 and 8.5 mrad; small angle calorimeters, Shashlyk type, covering below 1 mrad. The required γ detection inefficiency is lower than 10^{-5} above 10 GeV in the 1–8.5 mrad region, and within 10^{-3} down to 1 GeV. A cut at 35 GeV/c on the maximum π^+ momentum offline, to deal with π^0 of at least 40 GeV/c, and a sub-nanosecond time resolution are key requirements for the NA62 photon veto.

The LAV system consists of twelve rings placed in vacuum, surrounding the whole NA62 decay and detector regions in order to cover the required angles. Counters made of lead-glass blocks and phototubes from the electromagnetic calorimeter of the OPAL experiment [21] at LEP have been used to build the rings. Inefficiencies around 10^{-4} have been measured down to 0.5 GeV photons, using positrons at the Dafne Beam Test facility in Frascati (I) [17]. The first two rings have been successfully tested at CERN in 2009 and 2010. Eight rings are available in 2012 for the commissioning run.

Measurements based on samples of $K^+ \rightarrow \pi^+ \pi^0$ events, selected among the NA48 data, validated the LKr calorimeter performance as photon veto in NA62. The sub-nanosecond online time resolution makes this detector essential for triggering.

The muon detection system (MUV) will use an upgraded version of the NA48 hadronic calorimeter, completed with a new plane of fast pad-scintillators placed at the end of the apparatus, after an iron wall, for triggering purposes (MUV3). An online time resolution around 500–600 ps has been measured with test beams of a MUV3 prototype in 2010. Part of the MUV detector will also be tested in the 2012 run.

An integrated trigger and data acquisition system (TDAQ) has been developed to read-out most of the NA62 detector in a common way. The key element of the TDAQ system is the TEL62 board [22], an upgraded version of the LHC TELL1 [23]. Digitized signals from sub-detectors are asynchronously sent to a custom-made TDC board (TDCB) [22], housing the CERN HPTDC chip [24]. The TDCB sends leading and trailing time of the signals to the TEL62 module.

The trigger system should reduce the detector rate from 10 MHz to about 10 kHz, taking into account the event size and the available data bandwidth. A three-level trigger system will accomplish the task. No zero suppression of candidate events is foreseen due to the stringent requirements on veto efficiencies.

As a consequence, a Gbit/s data bandwidth capability will be essential for the whole trigger and read-out chain. The online sub-nanosecond time resolution required for the veto detectors and for the RICH are crucial features to avoid random veto and achieve efficiencies better than 95% for signals at the trigger level. For each sub-detector, the TEL62 processes the timing information, builds the trigger primitives implemented in firmware using the board's FPGA, and sends them to a central Level 0 trigger processor (L0TP). The L0TP processes these inputs with a latency time of about 1 ms, issues a trigger decision and sends it back to the TEL62. In case of a positive decision, the board allows the read-out of the data into dedicated detector PC's. The LKr uses Flash ADC instead of TDC, and two independent systems for trigger and read-out. The LKr, MUV3 and RICH detectors mainly contribute to the L0 trigger decisions, providing a rate suppression factor greater than 10.

The Level 1 and 2 trigger are based on PC's. The detector PC's process the 1 MHz data rate from the L0TP, send filtered data to a gigabit Ethernet switch and, later, to a PC farm which provides global event information for the final trigger decision. The raw data are finally assembled by dedicated event-building PC's and transferred to the Central Data Recording system for storing with a maximum speed of data logging on tape of about 100 MB/s.

In the first half of the year 2012 the available parts of the detector and of the TDAQ system have been installed along the NA62 beam line. An extensive test of the TDAQ system without beam took place in July and August 2012. About 6-week of data taking with beams will start in October for the commissioning of the detector and the TDAQ elements ready for use. The detector construction and installation will continue in 2013 and 2014, in view of the first physics run foreseen in fall 2014.

4. The R_K measurement

The concept of Lepton Flavour Universality (LFU), i.e. identical coupling constants for different lepton flavours, has naturally been built into the SM and is particularly well suited to verify the theory. The transition rates of leptonic and semi-leptonic meson decays proceeding via intermediate W^\pm boson exchange are carefully computed in terms of the Fermi coupling constant G_F and provide a powerful test of LFU. Since many extensions of the electroweak theory lead to violating universality for

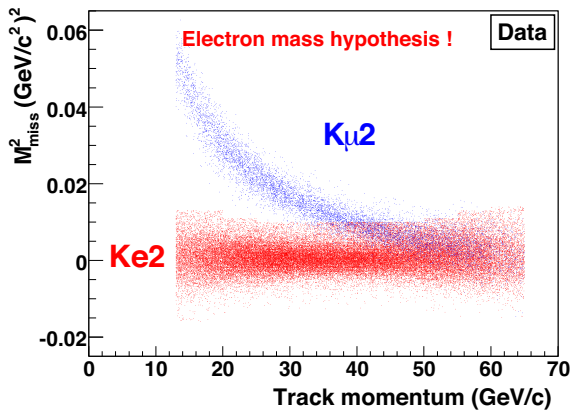


Fig. 4. Reconstructed K_{e2} and $K_{\mu 2}$ data samples: distribution of M^2_{miss} as a function of track momentum in the electron mass hypothesis.

different flavours, the precision measurements of those transition rates allow an accurate determination of fundamental electroweak parameters as well as a straightforward check of the SM predictions.

Precision tests of LFU are particularly significant in the case of the decays $P \rightarrow \ell \nu$ of pseudo-scalar mesons to light leptons, helicity-suppressed in the electroweak theory due to the $V-A$ structure of the charged current couplings. Remarkable progress has been made on the theoretical calculation of these processes, notably in the reduction of hadronic uncertainties due to the knowledge of non-perturbative quantities. Thanks to the availability of large amounts of experimental data, a relevant role is played by the measurements of the $\pi \rightarrow \ell \nu_\ell$ ($\pi_{\ell 2}$) and $K \rightarrow \ell \nu_\ell$ ($K_{\ell 2}$) leptonic decay rates, where $\ell = e$ or μ , and of their ratios $R_{K/\pi} \equiv \Gamma(K/\pi \rightarrow e \nu_e)/\Gamma(K/\pi \rightarrow \mu \nu_\mu)$.

The measurement of R_K , whose SM prediction is very accurate [25], as the main hadronic uncertainties cancel in the ratio, is particularly well suited to discriminate among new physics scenarios. Non-SM effects may actually induce pseudo-scalar currents and non-universal corrections to the lepton couplings, which could affect the R_K value, as predicted by multi-Higgs models, including the SUSY case [26].

The SM calculation of the ratio of the K_{e2} and $K_{\mu 2}$ decay widths including internal bremsstrahlung (IB) radiation, $R_K = \Gamma(K^\pm \rightarrow e \nu_e [\gamma])/\Gamma(K^\pm \rightarrow \mu \nu_\mu [\gamma])$, is [25]:

$$\begin{aligned} R_K^{SM} &= \left(\frac{M_e}{M_\mu}\right)^2 \left(\frac{M_K^2 - M_e^2}{M_K^2 - M_\mu^2}\right)^2 (1 + \delta R_{QED}) = \\ &= (2.477 \pm 0.001) \times 10^{-5} \end{aligned}$$

where $\delta R_{QED} = (-3.79 \pm 0.04)\%$ is an electromagnetic correction due to IB and structure-dependent effects and M_e , M_μ and M_K are, respectively, the electron, muon and kaon masses.

The low-energy minimal SUSY extension of the SM (MSSM) [26] allows non-vanishing e - τ mixing terms, mediated by charged Higgs bosons H^\pm , which could lead to a few percent enhancement of R_K , well within the current experimental sensitivity. In this case, R_K is sensitive to Lepton Flavour Violating (LFV) effects appearing at the one-loop level via the exchange of charged Higgs bosons H^\pm . The main contribution due to the LFV couplings of the H^\pm is:

$$R_K^{LFV} \approx R_K^{SM} \left[1 + \left(\frac{M_K}{M_H}\right)^4 \left(\frac{M_\tau}{M_e}\right)^2 \left|\Delta_R^{31}\right|^2 \tan^6 \beta \right]$$

where $\tan \beta$ is the ratio of the two Higgs vacuum expectation values and Δ_R^{31} is the mixing parameter between the superpartners of the right-handed leptons, which can reach a value of about 10^{-3} . This effect can enhance R_K by several percent without contradicting any experimental constraints known at present. The R_K measurement also represents a unique probe of mixing effects in the right-handed slepton sector [27] and is sensitive to the neutrino mixing parameters within the SM extension involving a fourth generation [28].

The ratio R_K was first measured in the 1970s. The current PDG [29] world average relies on a recent result from the KLOE collaboration [30]. A K_{e2} sample 10 times larger than the previous total world sample has been recorded by NA62 in 2007-08, exploiting an optimized set-up of the former NA48/2 detector and beam line. A sub-percent precision has been achieved by NA62 for this measurement [4][5].

4.1. The R_K measurement in NA62

The beam and the apparatus of the NA48/2 experiment [3] have been exploited for the R_K ratio measurement in NA62. The beam line was originally designed to deliver simultaneous K^+ and K^- beams produced by the 400 GeV/c protons from the CERN SPS. Single beam configurations with 74 GeV/c central momentum and 1.4 GeV/c rms spread were mostly used in 2007. The fiducial decay volume was contained in a 114 m long cylindrical vacuum tank.

The momenta of the charged decay products were measured in a magnetic spectrometer, housed in a tank filled with helium placed after the decay volume. The spectrometer consisted of four drift

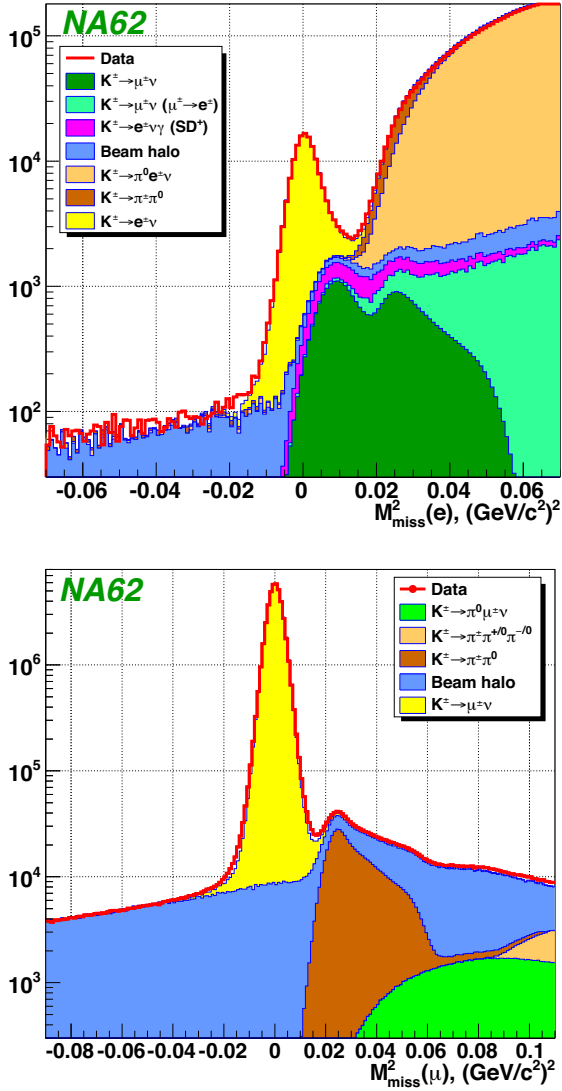


Fig. 5. Reconstructed M^2_{miss} distributions of the K_{e2} (top) and $K_{\mu2}$ (bottom) candidates compared with the sum of normalised estimated signal and background components.

chambers, two upstream and two downstream of a dipole magnet with a 265 MeV/c horizontal transverse momentum kick. Each chamber comprised eight planes of sense wires, oriented along the x, y and ± 45 degrees directions. The momentum resolution was $\Delta p/p = 0.48\% \oplus 0.009\% p$ (p in GeV/c).

A plastic scintillator hodoscope providing fast trigger signals and precise time measurements of charged particles was placed after the spectrometer.

The LKr electromagnetic calorimeter was used for lepton identification and as photon veto detector.

The analysis strategy is based on counting the numbers of reconstructed K_{e2} and $K_{\mu2}$ candidates, collected concurrently. The study is performed independently for 40 separated data samples (10 bins of reconstructed lepton momenta and 4 samples with different data taking conditions) by computing R_K as:

$$R_K = \frac{1}{D} \cdot \frac{N(K_{e2}) - N_B(K_{e2})}{N(K_{\mu2}) - N_B(K_{\mu2})} \cdot \frac{A(K_{\mu2})}{A(K_{e2})} \cdot \frac{f_\mu \times \varepsilon(K_{\mu2})}{f_e \times \varepsilon(K_{e2})} \cdot \frac{1}{f_{LKr}}$$

where ($\ell = e, \mu$): $N(K_{\ell2})$ are the numbers of $K_{\ell2}$ candidates; $N_B(K_{\ell2})$ are the numbers of background events; $A(K_{\ell2})$ are the geometric acceptances; f_ℓ are the lepton identification efficiencies; $\varepsilon(K_{\ell2})$ are the trigger efficiencies; f_{LKr} is the global efficiency of the LKr read-out, affecting only the K_{e2} selection; $D = 150$ is the $K_{\mu2}$ trigger downscaling factor.

The analysis does not rely on the measurement of the absolute beam fluxes and several systematic effects cancel in the ratio, at the first order. A detailed Monte Carlo simulation based on Geant3 [15] is used to evaluate the signal geometric acceptances $A(K_{\ell2})$ and the geometric acceptances for the background processes used in the calculation of $N_B(K_{\ell2})$. Particle identification, trigger and read-out efficiencies are measured directly from the data.

Two selection criteria are used to distinguish between K_{e2} and $K_{\mu2}$ decays. The kinematic identification is based on the reconstructed squared missing mass $M^2_{\text{miss}}(\ell) = (P_K - P_\ell)^2$, where P_K and P_ℓ ($\ell = e, \mu$) are the kaon and lepton 4-momenta, assuming the track to be an electron or a muon. Figure 4 illustrates the kinematic separation of the K_{e2} and $K_{\mu2}$ samples. A selection condition is applied, $-M^2_1 < M^2_{\text{miss}}(\ell) < M^2_2$, where M^2_1 and M^2_2 vary across the lepton momentum bins depending on resolution. Lepton type identification is based on the ratio E/p between the LKr calorimeter energy deposit and the track momentum measured by the spectrometer. Particles with $(E/p)_{\text{min}} < E/p < 1.1$ ($E/p < 0.85$) are identified as electrons (muons). Depending on momentum, $(E/p)_{\text{min}}$ is 0.90 or 0.95.

The largest background to the K_{e2} sample is the $K_{\mu2}$ decay with a μ misidentified as an electron ($E/p > 0.95$), due to the μ -bremsstrahlung process in the LKr. To reduce the corresponding uncertainty, the μ misidentification probability has been measured as a function of momentum with dedicated data samples.

The numbers of selected K_{e2} and $K_{\mu2}$ candidates are, respectively, 145,958 and 4.2817×10^7 (the latter selected through a pre-scaled trigger). The squared

missing mass $M_{\text{miss}}^2(\ell)$ of the $K_{\ell 2}$ candidates ($\ell = e, \mu$) and the backgrounds are shown in Figure 5.

The result of the measurement, combined over all the 40 independent samples taking into account correlations of the systematic errors, is [4]:

$$R_K = (2.488 \pm 0.007_{\text{stat.}} \pm 0.007_{\text{syst.}}) \times 10^{-5} \\ = (2.488 \pm 0.010) \times 10^{-5}$$

The stability of the result has been checked in lepton momentum bins for all separated data samples. The systematic error includes uncertainties on the backgrounds, the spectrometer alignment, the helium purity in the spectrometer tank, the beam simulation and effects due to particle identification and trigger efficiency. The uncertainties of the combined result are summarised in Table 1. The background contributions to the K_{e2} sample, integrated over lepton momenta, have been estimated with Monte Carlo simulations, except for the beam halo one which was measured directly with dedicated data samples.

The NA62 measurement of the R_K ratio is the most precise to date; it is consistent with the KLOE results [30] and with the SM expectation [25] and can be used to constrain multi-Higgs [26] and fourth generation [28] new physics scenarios.

Table 1. Summary of the R_K uncertainties.

SOURCE	$\delta R_K \times 10^5$
STATISTICAL	0.007
$K_{\ell 2}$ background	0.004
$K^{\pm} \rightarrow e^{\pm} \nu_e \gamma$ (SD ⁺)	0.002
$K^{\pm} \rightarrow \pi^0 e^{\pm} \nu_e$ and $K^{\pm} \rightarrow \pi^0 \pi^{\pm}$	0.003
Beam halo background	0.002
He purity	0.003
Acceptance correction	0.002
Spectrometer alignment	0.001
Positron identification	0.001
1-track trigger efficiency	0.001
LKr read-out efficiency	0.001
TOTAL	0.010

5. Conclusions

A challenging experimental program is going on in the framework of the NA62 project at CERN. The construction and installation of the detector is well progressing toward the physics runs expected in 2014 and 2015, after the CERN accelerator shutdown. A commissioning run is taking place in 2012 with the available sub-detectors and TDAQ elements.

Based on an early experimental set-up, NA62 performed the measurement of the ratio R_K with the unprecedented uncertainty of 0.4%. However, this accuracy is still one order of magnitude bigger than the SM one and further improvements are expected with the data of the new physics runs.

In addition to the NA62 main goal, as already experienced in NA48, the performance of the new detector and the increased data statistics will allow to address in the near future an enlarged interesting physics program, based on the improvement of measurements of rare and forbidden K^{\pm} decays and of fundamental physics parameters.

References

- [1] G. Anelli et al., CERN-SPSC-2005-013, CERN-SPSC-P-326 (2005).
- [2] The NA62 Collaboration, CERN-SPSC-2007-035, SPSC-M-760 (2007).
- [3] V. Fanti et al., Nucl. Instrum. Method A574, 433 (2007).
- [4] E. Goudzovski, [arXiv:1208.2885v1[hep-ex]] (2012).
- [5] C. Lazzeroni et al., Phys. Lett. B698, 105 (2011).
- [6] J. Brod, M. Gorbahn and E. Stamou, Phys. Rev. D83 (2011) 034030, [arXiv:1009.0947 [hep-ph]].
- [7] S.L. Glashow, J. Iliopoulos, L. Maiani, Phys. Rev. D2 (1970) 1285.
- [8] C. Smith, [arXiv:1012.3698v1[hep-ph]], 2010.
- [9] Y. Grossman and Y. Nir, Phys. Lett. B398 (1997) 163, [arXiv:9701313[hep-ph]].
- [10] A.V. Artamonov et al., Phys. Rev. D79 (2009) 092004, [arXiv:0903.0030[hep-ph]].
- [11] J. K. Ahn et al., Phys. Rev. D81 (2010) 072004, [arXiv:0911.4789v2[hep-ex]].
- [12] E. Iwai, these proceedings.
- [13] E.T. Worcester, these proceedings.
- [14] S. Agostinelli et al., Nucl. Instrum. Method A506, 250 (2003).
- [15] CERN Program Library Long Writeup, W5013 (1993).
- [16] A. Ferrari, P.R. Sala, A. Fasso and J. Ranft, CERN-2005-010.
- [17] The NA62 Collaboration, Technical Design (2010), <http://na62.web.cern.ch/NA62/Documents/TechnicalDesign.html>.
- [18] M. Bovet et al., CERN Report: CERN 82-13 (1982).
- [19] G. Anzivino et al., Nucl. Instrum. Method A593, 314 (2008).
- [20] B. Angelucci et al., Nucl. Instrum. Method A621, 205 (2010).
- [21] K. Ahmet et al., Nucl. Instrum. Method A305, 275 (1991).
- [22] C. Avanzini et al., Nucl. Instr. and Method A623 (2010) 543.
- [23] G. Haefeli et al., Nucl. Instrum. Method A560, 494 (2006).
- [24] J. Christiansen, "HPTDC High Performance Time to Digital Converter", CERN, Geneva, 2004, Version 2.2 for HPTDC version 1.3.
- [25] V. Cirigliano and I. Rosell, Phys. Rev. Lett. 99, 231801 (2007).
- [26] A. Masiero, P. Paradisi and R. Petronzio, Phys. Rev. D 74 011701 (2006); J. High Energy Phys. 0811 042 (2008).
- [27] J. Ellis, S. Lola and M. Raidal, Nucl. Phys. B812, 128 (2009).
- [28] H. Lacker, A. Menzel, J. High Energy Phys. 1007 006 (2010).
- [29] K. Nakamura et al., J. Phys G3, 075021 (2010).
- [30] F. Ambrosino et al., Eur. Phys. J. C64, 627 (2009); Eur. Phys. J. C65, 703 (2010).